Supporting Information

for

Templated synthesis of a bifunctional Janus graphene for enhanced enrichment of both organic and inorganic targets

Kang Yuan[a,b], Yong Li[a], Xiu Huang[a,c], Yong Liang[b], Qian Liu[a,b,c,*], Guibin Jiang[a,c]

[a] *State Key Laboratory of Environmental Chemistry and Ecotoxicology, Research Center for Eco-Environmental Sciences, Chinese Academy of Sciences, Beijing 100085, China*

[b] *Institute of Environment and Health, Jianghan University, Wuhan 430056, China*

[c] *College of Resources and Environment, University of Chinese Academy of Sciences, Beijing 100190, China*

Email: qianliu@rcees.ac.cn

Content

1. Experimental section
2. Supporting tables
3. Supporting figures
4. References for SI

1. Experimental section

1.1. Chemicals and reagents

N,*N*-Dimethylformamide (DMF), *N*,*N*′-dicyclohexylcarbodiimide (DCC), silica micropowder and octadecylamine (ODA) were purchased from Aladdin (Shanghai, China). Graphene and graphene oxide (GO) dispersions (Single layer ratio = 99%) were bought from XFNANO (Nanjing, China). 3-Aminopropyl-triethoxysilane (APTES) was purchased from Acros Organics (Beijing, China). *N*-[(3-Trimethoxysilyl)propyl]ethylenediamine triacetic acid trisodium salt (EDTA-silane) was bought from J&K Scientific Ltd. (Beijing, China). Toluene, ethanol, methanol, KOH and ethyl ether were purchased from Sinopharm Chemical Reagent Beijing Co. (Beijing, China). Bisphenol S (BPS), tetradecyldimethylbenzylammonium chloride hydrate (TDBAC), and tetrabromobisphenol A (TBBPA) were from TCI (Tokyo, Japan). Perfluorooctanesulfonate (PFOS) and 2,2′,4,4′-tetrabromodiphenyl ether (BDE-47) were from AccuStandard (New Haven, CT, USA.). Estradiol (E2) and pentachlorophenol (PCP) were purchased from Dr. Ehrenstorfer (Augsburg, Germany). Dodecyldimethylbenzylammonium chloride (DDBAC), cetyltrimethylammonium bromide (CTAB), tetradecyltrimethylammonium bromide (TTAB) and α-cyano-4-hydroxycinnamic acid (CHCA) were from Sigma (St. Louis, MO). Standard Pb(II) solution (1 mg/mL Pb(II) in 1 mol/L HNO_3) was bought from General Research Institute for Nonferrous Metals (Beijing, China). Ultrapure water from Milli-Q system (Millipore, Billerica, MA) was used throughout. All reagents were of analytical grade.

1.2. Synthesis of GO-encapsulated silica particles (SiO_2@GO)

First, monodisperse SiO_2 microspheres were functionalized with APTES by using the previously reported method.[1] The SiO_2 microspheres (5 g) were dispersed in 200 mL of dry toluene with the aid of ultrasonication, followed by the addition of 2.5 mL of APTES. The mixture was stirred and refluxed at 95 °C for 24 h to obtain amino-functionalized SiO_2 (SiO_2-NH_2). The obtain SiO_2-NH_2 particles were centrifuged, washed with ethanol and deionized water three times, and freeze-dried under vacuum.

Second, single-layer GO sheets were assembled onto the SiO_2-NH_2 spheres as previously reported.[2] The SiO_2-NH_2 (1 g) was dispersed in 100 mL of deionized water with ultrasonication. Then, 100 mL of single-layer GO dispersion (0.2 mg/mL) was slowly added into the SiO_2-NH_2 aqueous suspension under mechanical stirring for 3 h at room temperature. After the reaction finished, SiO_2@GO particles were precipitated at the bottom of the flask. The precipitates

(SiO_2@GO) were collected and washed with deionized water to remove the unbound GO, and then freeze-dried.

1.3. Synthesis of Janus graphene (C_{18}-GO-EDTA)

The as-prepared SiO_2@GO was first single-sided functionalized with EDTA-silane. Briefly, SiO_2@GO (1 g) was added to a three-neck flask containing 200 mL of ethanol and dispersed by the aid of ultrasonication for 1 h. Then, 3 mL of 40% EDTA-silane aqueous solution was added. The mixture was refluxed and stirred for 24 h at 65 °C. Afterwards, 100 mL of methanol was added to dislodge the unreacted EDTA-silane.[3] The product (SiO_2@GO-EDTA) was obtained by centrifugation and washed with methanol and water repeatedly, and freeze-dried under vacuum.

Then, the SiO_2 core was etched by KOH solution.[4] The SiO_2@GO-EDTA (0.5 g) was chemically etched in 100 mL of KOH solution (5 mol/L) for 4 d at 80 °C. Eventually, the single-sided functionalized graphene (GO-EDTA) was obtained by centrifugation and filtration to remove the residual silica and K_2SiO_3, and then washed with deionized water and freeze-dried.

Finally, octadecylamine (ODA) was asymmetrically modified onto the other side of GO-EDTA. The GO-EDTA (20 mg) was dispersed in 5 mL of deionized water by the aid of sonication for 30 min. The dispersion was loaded into a flask containing 50 mL of DMF, and then ODA (300 mg) and DCC (40 mg) were added. The mixture was heated under stirring at 70 °C for 24 h. After reaction, the suspension was centrifugated at 12000 rpm for 30 min to precipitate the final product Janus graphene (C_{18}-GO-EDTA). The product was purified by redispersion in ethyl ether and centrifugation followed by freeze-dried under vacuum. The yield of JG is estimated by

$$\text{Yield} = \frac{m_{JG}}{m_{GO}/f_{GO}} \times 100\% \quad (1)$$

where m_{JG} is the mass of final product JG, m_{GO} is the mass of raw material GO, and f_{GO} is the mass percentage of GO component in the JG. The m_{JG} and m_{GO} can be directly obtained in the experiments, and the f_{GO} can be estimated from the atomic percentages given by the XPS measurements (see Table S1 and Section 1.10 in SI) to be 0.70. In this way, the yield of JG in this study was estimated to be 37.1%.

Such a yield means that a portion of GO was lost during the synthesis and thus further technical improvement in the synthesis may be required. In addition, although the synthesis was carried out only with 20 mg of GO, considering that all reactions were processed in bulk

solution and no special devices were used, this synthesis should be easily scaled up to gram- or larger scales.

1.4. Characterization of materials

FE-TEM images were taken on a Hitachi JEM-2100F field-emission transmission electron microscope (Tokyo, Japan). High-resolution SEM images were captured on a Hitachi SU-8020 field-emission scanning electron microscope (Tokyo, Japan). AFM images were captured on an Agilent 5500 Atomic Force Microscope (Santa Clara, CA). The AFM samples were deposited on a fresh mica wafer. The samples were prepared in ultrapure water at a concentration of 10 mg/L. An aliquot (20 μL) of the sample was deposited to a fresh mica wafer and air-dried at room temperature. Zeta potentials were measured on a Nano-ZS zetasizer (Malvern Instruments, Worcestershire, UK). FT-IR spectra were obtained on a JASCO FT-IR Fourier transform infrared spectrometer (Victoria, B. C., Canada). The samples were mixed and ground with KBr and then pressed into transparent disks for measurement. XPS spectra were obtained by using a Thermo Scientific Escalab 250Xi X-ray photoelectron spectrometer (Massachusetts, USA) with Al Kα X-ray radiation as the X-ray source excitation.

1.5. MALDI-TOF MS analysis

For MALDI-TOF MS analysis, the sample solution and the matrix dispersion were mixed at a ratio of 1:1 (v/v), and 2 μL of the mixture was placed onto a stainless steel MTP target frame III (Bruker Daltonics) followed by air drying. Reflector mode was used for the analysis of low-mass compounds. A 355 nm Nd:YAG laser with the frequency of 100 Hz was used, and the laser power was set to 20%. In MALDI-TOF MS analysis, the same intensity of the incident light was used for each sample to ensure a fair comparison among different materials. The spectra were recorded by summing 200 laser shots. The data processing was performed with the FlexAnalysis 3.0 software.

1.6. SELDI-TOF MS analysis

For SELDI-TOF MS analysis, human whole blood samples were used as the target complex media. The human whole blood samples were obtained from the Second Hospital of Tianjin Medical University (Tianjin, China) and stored at -20 °C. The probe material was dispersed in water at 2 mg/mL by the aid of ultrasonication. After that, a single drop of human whole blood sample (20 μL) was diluted in 900 μL of water and then 100 μL of the probe dispersion (2 mg/mL) was added to enrich the target analytes. The mixture was incubated in a shaking table at room temperature for 2 h. Then the sediment was collected by centrifugation

at 10000 rpm for 15 min. Finally, 2 μL of the sediment was deposited onto the MALDI target for analysis. Reflector mode was used for the analysis of low-mass compounds. A 355 nm Nd:YAG laser with the frequency of 100 Hz was used, and the laser power was set to 40%. In SELDI-TOF MS analysis, the same intensity of the incident light was used for each sample. The spectra were recorded by summing 200 laser shots.

1.7. ICP-MS measurement

For ICP-MS measurement, the sample solution was diluted by 5% HNO_3. The standard curve was established in the range of 0-150 μg/L. The Pb(II) concentration was detected with Sc as an interior standard element. The Ni(II) concentration was detected with In as an interior standard element.

1.8. HPLC-ESI-MS/MS analysis

The HPLC-ESI-MS/MS system consisted of an UltiMate™ 3000 DGLC high-performance liquid chromatograph (ThermoFisher Scientific, USA) and a TSQ Quantiva triple quadrupole mass spectrometer (ThermoFisher Scientific). The sample (10 μL) was injected into an Acclaim 120 column (5 μm, 100 Å, 150 mm × 4.6 mm, ThermoFisher Scientific). Ammoniom acetate (10 mM, pH 4; A) and acetonitrile (B) were used as the mobile phases. The flow rate was set at 1 mL/min. The dual mobile-phase gradient started at 10% B; held constant for 1.5 min; changed to 95% B by 4 min; remained constant until 8 min; returned to the initial condition by 8.5 min; and then balanced for 1.5 min.

1.9. Adsorption experiment

To perform adsorption isotherm analysis of metal ions, 0.1 mg of the adsorbent (Janus graphene or GO) was added to a Pb(II) or Ni(II) solution (1 mL) at room temperature. The initial concentration varied from 5 to 250 mg/L. The pH value of Pb(II) and Ni(II) solutions was ~1.5 and ~6.5, respectively. Then, the mixture was oscillated in a shaking table at 25 °C for 24 h to achieve adsorption equilibrium. Finally, the supernatant was collected by centrifugation at 12000 rpm for 30 min. The Pb(II) or Ni(II) concentration in the supernatant was detected by ICP-MS (Agilent 8800).

For adsorption isotherm analysis of PFOS, the adsorbent (Janus graphene or GO) was dispersed in water at 1 mg/mL by the aid of ultrasonication. Then, PFOS was dissolved in 900 μL of water and then 100 μL of the dispersions (1 mg/mL) was added. The initial concentrations varied from 0.05 to 10 mg/L. The mixture was oscillated in a shaking table at 25℃ for 24 h. After that, the supernate was collected by centrifugation at 12000 rpm for 30 min. Finally, the

supernate was diluted to 0.5 mL for HPLC-ESI-MS/MS analysis.

1.10. Estimate of ratio of ODA to EDTA-silane in JG

The JG consists of three components, GO, ODA, and EDTA-silane. From the atomic percentages given by XPS (Table S1), we can roughly estimate the molar ratio of ODA to EDTA-silane in JG.

First, providing all of the Na in JG is from EDTA-silane (no other Na-containing reagents are used in the synthesis), we can obtain the atomic percentages of EDTA-silane in JG (Na: 0.75%; C: 3.25%; O: 2.00%, N: 0.50%). Note that SiO_2 is used as a template in the synthesis and that JG may have residual Si, so Si is not used in the estimation. After subtracting the EDTA-silane component from JG, we can obtain the atomic percentages contributed by GO and ODA to JG (C: 65.80%; O: 22.95%, N: 2.93%). Considering that ODA contains no O, the C/O atomic ratio contributed by GO and ODA ($R_{C/O}$) in JG can be given by

$$R_{C/O} = \frac{C_{GO} + C_{ODA}}{O_{GO}} = \frac{65.80\%}{22.95\%} \quad (2)$$

where C_{GO} and C_{ODA} are the C contributed by GO and ODA in JG, respectively, and O_{GO} is the O contributed by GO in JG. From Table S1, the C/O atomic ratio of GO ($R_{C/O}$') is

$$R_{C/O}' = \frac{C_{GO}}{O_{GO}} = \frac{64.88\%}{32.59\%} \quad (3)$$

From Eqs. 2 and 3, we can obtain $C_{GO}/C_{ODA} = 2.27$. Since the total C contributed by GO and ODA to JG is 65.80%, we can obtain that the C contributed by GO and ODA are 45.68% and 20.12%, respectively. Then, we can obtain

$$\frac{C_{ODA}}{C_{EDTA\text{ - }silane}} = \frac{20.12\%}{3.25\%} = 6.2 \quad (4)$$

where $C_{EDTA\text{-}silane}$ is the C contributed by EDTA-silane in JG. Taking into account the atomic number of C in an ODA ($C_{18}N$; n = 18) or EDTA-silane ($C_{13}O_8N_2Na_3Si$; n = 13) molecule, we can finally estimate the molar ratio of ODA to EDTA-silane in the JG to be:

$$R_{ODA/EDTA-silane} = \frac{C_{ODA}/18}{C_{EDTA-silane}/13} = 4.5 \quad (5)$$

That is, the loading molar ratio of ODA to EDTA-silane in the JG is estimated to be 4.5:1.

2. Supporting tables

Table S1. Atomic percentages of GO and JG from the XPS measurements.[a]

element	atomic percent (%)	
	GO	JG
C	64.88	69.05
O	32.59	24.95
N	2.52	3.43
Na	0	0.75
Si	0	1.81

[a] The JG consists of three components, GO, ODA, and EDTA-silane. From the atomic percentage data, we can roughly estimate the molar ratios of GO, ODA, and EDTA-silane in JG (see the Section 1.10 in SI). Result shows that the loading ratio of ODA to EDTA-silane in JD is 4.5:1. This value suggests that the JG is not a "perfect" Janus material. The amount of ODA is estimated to be higher than that of EDTA. This can be explained by the fact that the ODA-functionalization is later than the EDTA-functionalization, so the EDTA side may be partly modified by ODA if the coverage by EDTA is incomplete.

Table S2. Results and parameters associated with the Langmuir model for the adsorption of metal ions on JG and GO.[a]

ion	material	Langmuir model parameter		
		q_{max} (mg/g)	K_l (L/mg)	R^2
Pb(Ⅱ)	Janus graphene	256	5.33×10^{-3}	0.874
	Graphene oxide	105	1.06×10^{-2}	0.896
Ni(Ⅱ)	Janus graphene	300	8.51×10^{-3}	0.876
	Graphene oxide	125	5.01×10^{-3}	0.682

[a] Langmuir model: $\frac{1}{q_e}=\frac{1}{q_{max}}+\frac{1}{q_{max}K_1C_e}$

where q_e (mg/g) is the adsorption amount of target on adsorbent at the equilibrium state, q_{max} (mg/g) is the adsorption capacity of target on adsorbent, C_e (mg/L) is the equilibrium concentration of target, K_l is the Langmuir adsorption constant that is associated with the adsorption energy.[5]

Table S3. Results and parameters associated with the Langmuir model for the adsorption of PFOS on JG and GO.[a]

compound	material	Langmuir model parameter		
		q_{max} (mg/g)	K_l (L/mg)	R^2
PFOS	Janus graphene	30	0.604	0.98
	Graphene oxide	12	0.307	0.952

[a] The definition of parameters are the same as in Table S2.

Table S4. Feature peaks and LODs (S/N = 3) of organic targets obtained with different materials as SELDI probes in analysis of single-drop human whole blood samples.

compound	*m*/*z*	LOD (pg/mL)		
		JG	G	GO
BPS	248.4	2	100	1.0×10^3
BDE-47	250.2	50	5.0×10^3	1.0×10^3
PCP	264.2	10	100	100
E2	270.5	50	5.0×10^3	5.0×10^3
PFOS	498.5	1	1	2
TBBPA	542.4	10	500	5.0×10^3
TTAB	255.9	50	500	500
CTAB	284.0	5	500	500
DDBAC	304.0	10	100	1.0×10^3
TDBAC	332.1	10	2.0×10^3	1.0×10^3

Table S5. Reproducibility test of the MALDI- and SELDI-TOF methods with different materials as matrices or probes.

compound	shot-to-shot RSD (n = 20)[a]			sample-to-sample RSD (n = 15)[b]		
	graphene matrix[c]	JG matrix[d]	whole blood sample[e]	graphene matrix[c]	JG matrix[d]	whole blood sample[e]
BPS	53.1%	22.7%	26.3%	60.9%	22.9%	22.8%
BDE-47	68.5%	29.9%	30.7%	78.1%	34.2%	26.3%
PCP	66.2%	32.5%	18.5%	82.5%	33.3%	25.5%
E2	53.2%	17.4%	17.9%	65.7%	17.6%	22.7%
PFOS	72.6%	31.5%	12.4%	73.7%	24.7%	20.1%
TBBPA	57.5%	23.7%	21.0%	69.9%	51.9%	26.2%
TTAB	36.6%	9.8%	10.6%	31.2%	19.2%	11.0%
CTAB	53.1%	9.4%	10.0%	37.3%	22.7%	10.0%
DDBAC	39.7%	11.5%	15.7%	34.7%	23.3%	17.0%
TDBAC	50.0%	13.1%	16.6%	35.8%	32.2%	16.7%

[a] The shot-to-shot RSDs were measured based on 20 shots at different locations on the matrix. [b] The sample-to-sample RSDs were measured based on 15 samples in different batches. [c] The RSDs were obtained in MALDI-TOF MS analysis of the mixed standard with graphene as a matrix. [d] The RSDs were obtained in MALDI-TOF MS detection of the mixed standard with Janus graphene as a matrix. [e] The RSDs were obtained in analysis of human whole blood samples by using Janus graphene as a SELDI probe.

3. Supporting figures

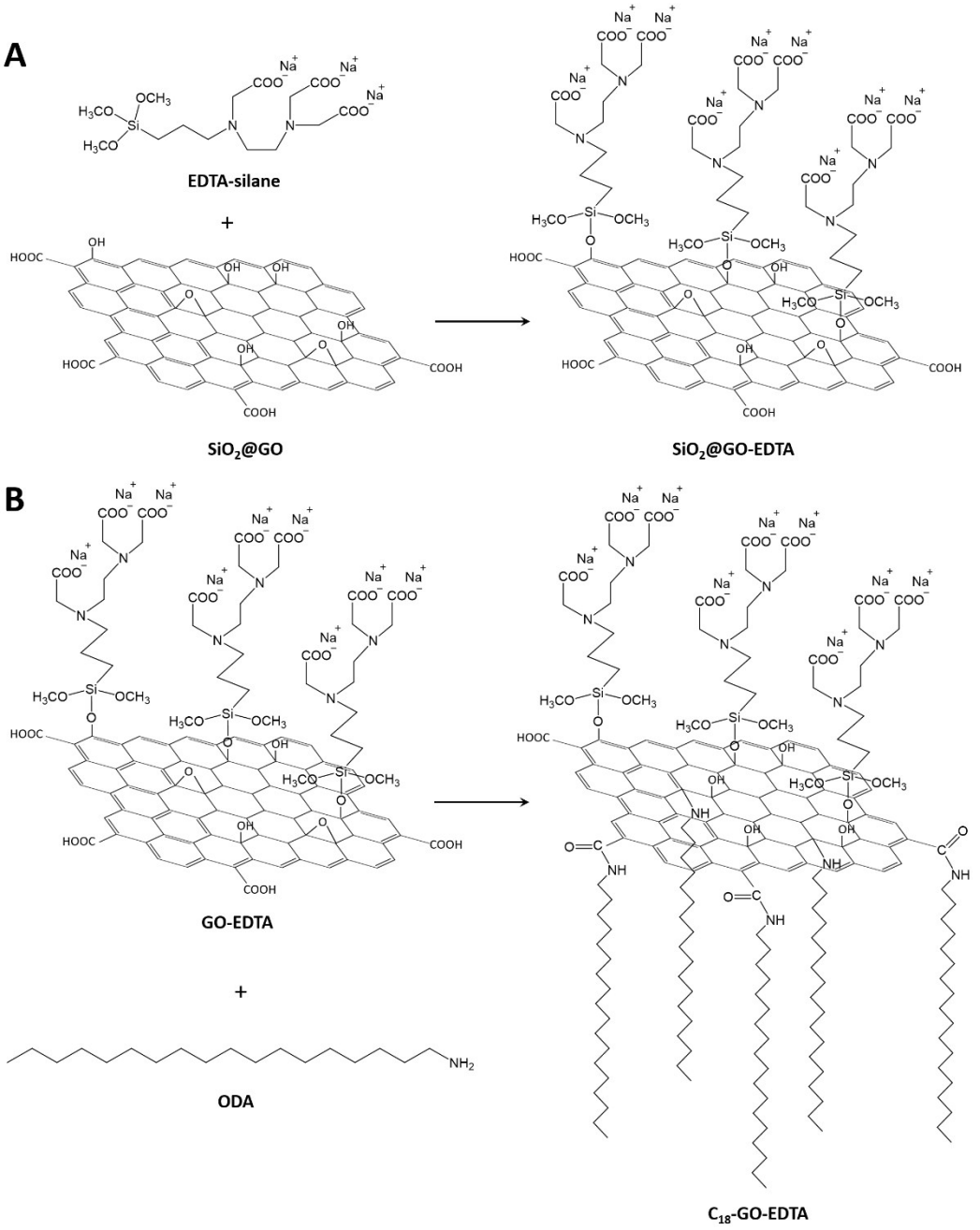

Fig. S1. The key reaction formulas in the synthesis of JG. (**A**) Synthesis of SiO_2@GO-EDTA via the interaction of EDTA-silane with hydroxyl groups at the SiO_2@GO surface. Note that the SiO_2 microsphere is not shown in the formula. (**B**) Synthesis of C_{18}-GO-EDTA by asymmetrically covalent bonding of ODA to the other side of the GO-EDTA sheets. The ODA can be covalently bonded to GO-EDTA via amidation with carboxylic groups or nucleophilic substitution with epoxy groups at the GO surface.

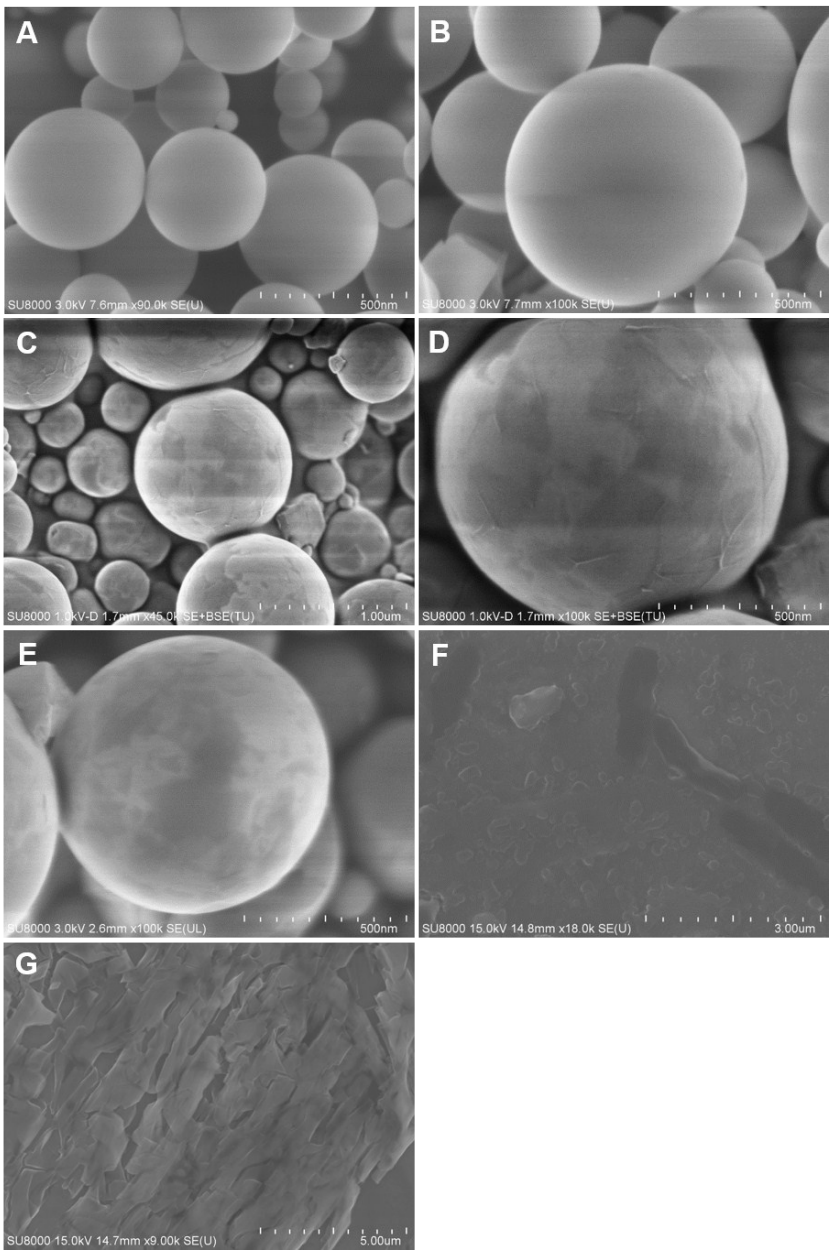

Fig. S2. Field-emission SEM (FE-SEM) images of (**A**) SiO_2 microspheres, (**B**) SiO_2-NH_2, (**C**, **D**) SiO_2@GO, (**E**) SiO_2@GO-EDTA, (**F**) GO-EDTA, and (**G**) Janus graphene. (**D**) is a high-resolution image of SiO_2@GO. From (**A**), the SiO_2 microspheres were near-monodispersed and the size was 200-600 nm. From (**B**), after aminated reaction, no obvious change in morphology was observed. From (**C**) and (**D**), the microspheres were tightly encapsulated by plicated and single-layer GO sheets. From (**E**), after the EDTA-silane modification, the microspheres were still tightly encapsulated by GO sheets. From (**F**), the SiO_2 microspheres were entirely etched by KOH solution, and all GO-EDTA sheets were successfully peeled off. From (**G**), the final product JG maintained a nanosheet morphology as GO.

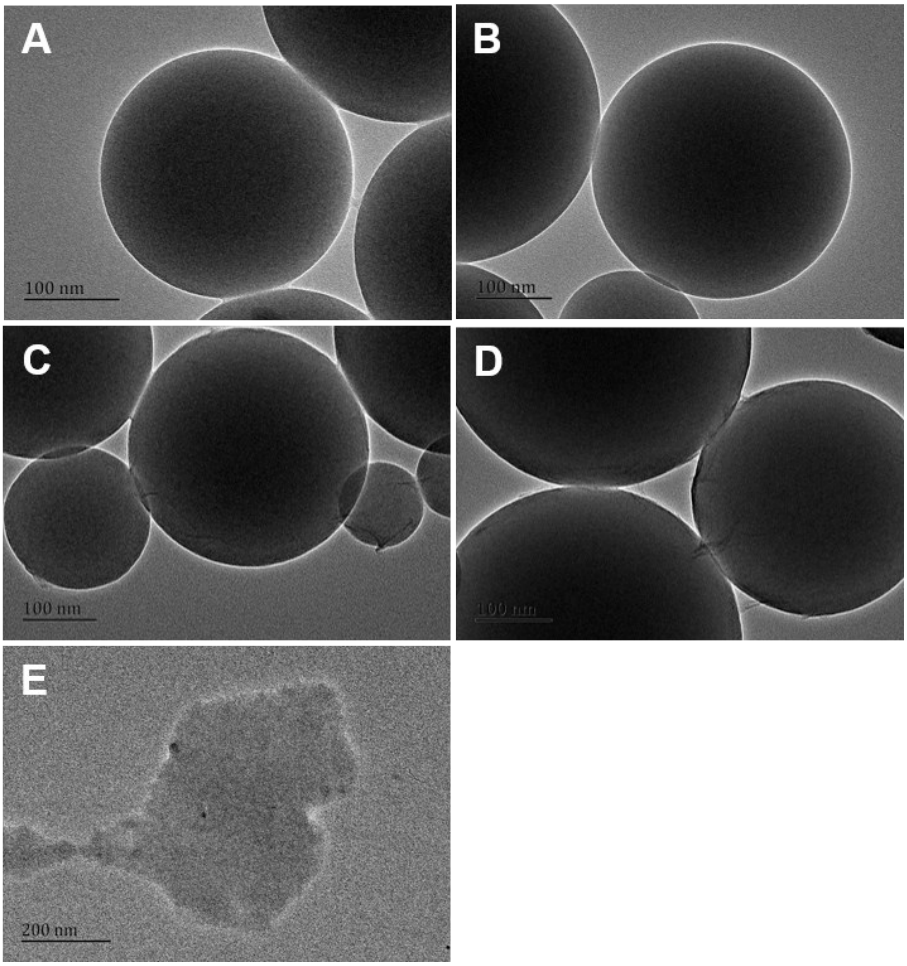

Fig. S3. FE-TEM images of (**A**) SiO_2, (**B**) SiO_2-NH_2, (**C**) SiO_2@GO, (**D**) SiO_2@GO-EDTA, and (**E**) GO-EDTA. The results were similar with those in the FE-SEM measurements (Fig. S2) and validated the effectiveness of the synthetic strategy.

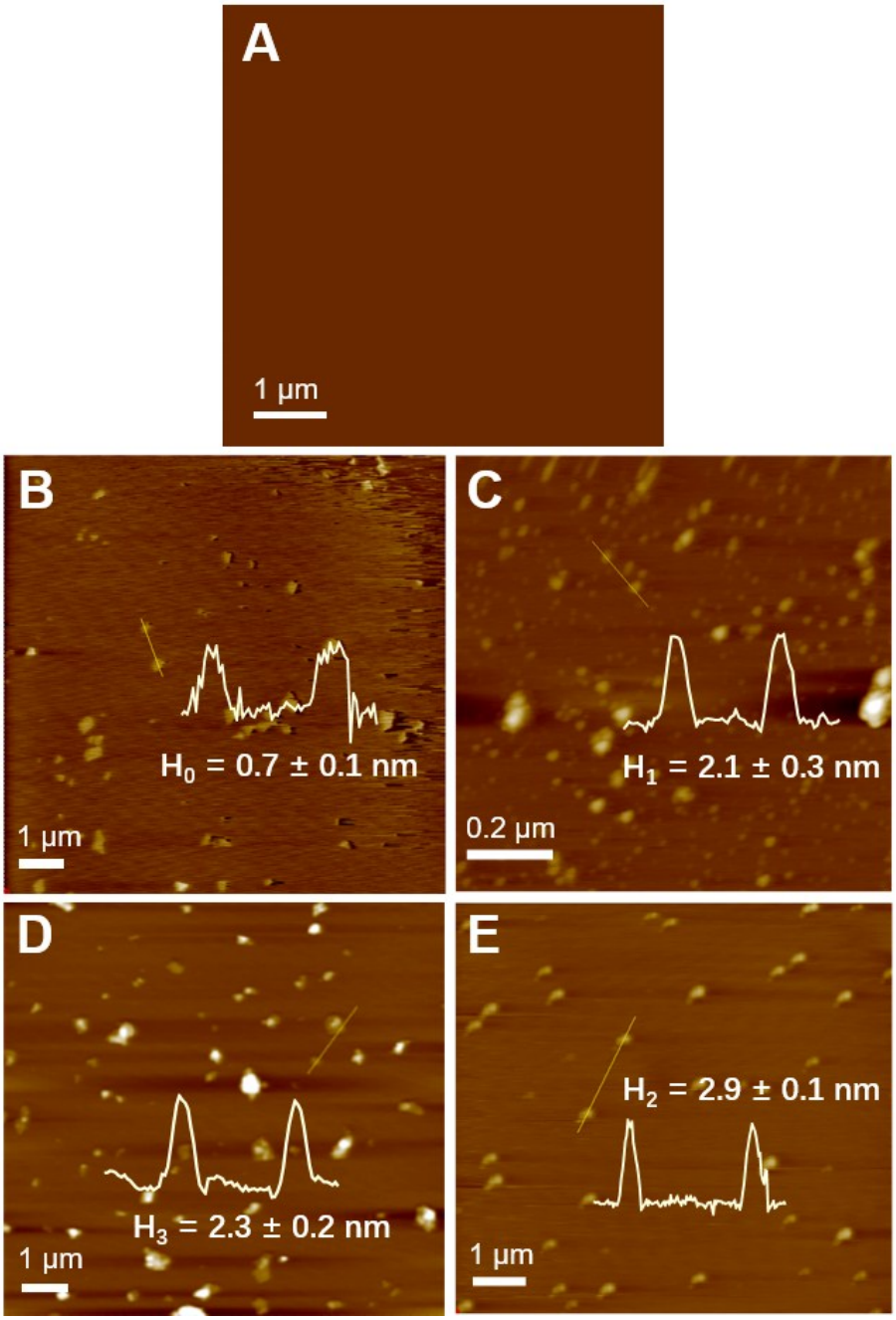

Fig. S4. High-resolution AFM images of bare substrate with the solvent alone (**A**), GO (**B**), GO-EDTA (**C**), two-sided symmetrical functionalized C_{18}-GO-C_{18} (**D**), and two-sided asymmetrical functionalized C_{18}-GO-EDTA (**E**). The error bars of height are estimated based on different sheets excluding large aggregates (n = 16). As shown in (**A**), the control experiment with the solvent alone indicated that no contamination or residues were present in the AFM imaging.

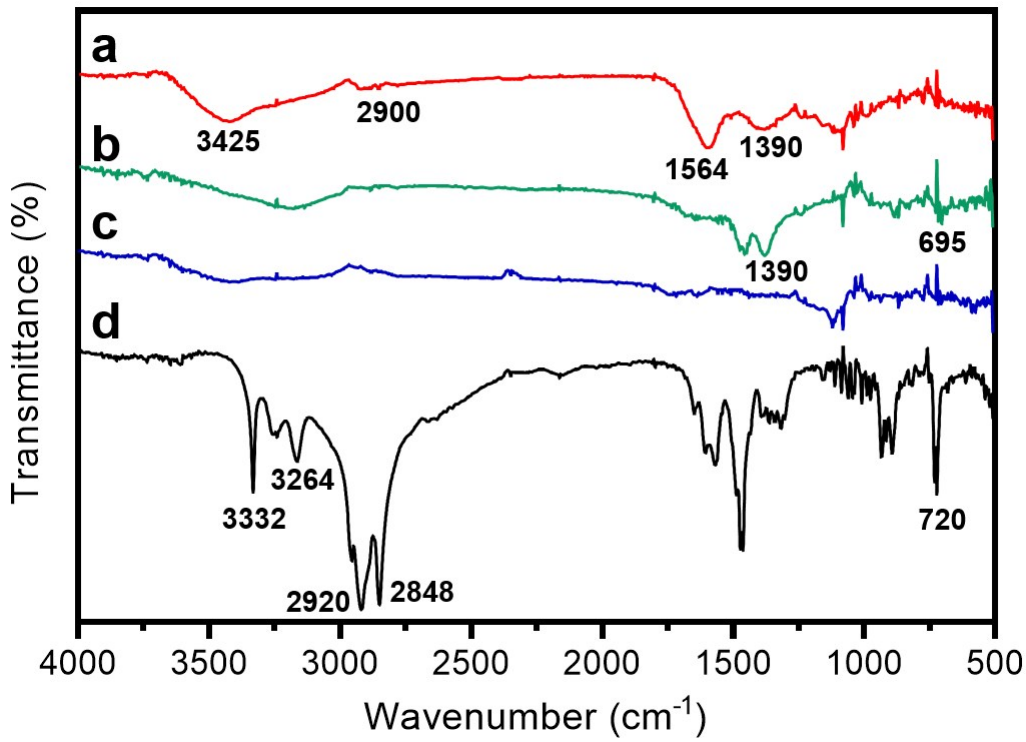

Fig. S5. High-solution FT-IR spectra of JG (**a**), GO-EDTA (**b**), GO (**c**), and ODA (**d**). The absorption at 695 cm^{-1} in GO-EDTA corresponds to the stretching vibrations of the C-O-Si. The new peak at 1390 cm^{-1} in **a** and **b** is ascribed to the γ_{CH_2} group of EDTA. In the spectrum of JG (**a**), the absorption at 2900 cm^{-1} is due to the C-H stretching of the octadecyl chain. Moreover, the peak at 1564 cm^{-1} corresponding to the N-H stretching vibration is observed, manifesting the formation of C-NH-C bond. The reaction is also evidenced by the disappearance of the peaks of primary amine group at 3332 and 3264 cm^{-1} (**d**) and the occurrence of a peak of secondary amine at 3425 cm^{-1}. The peak at 695 cm^{-1} in GO-EDTA nearly disappears for the JG probably due to the influence of the peak at 720 cm^{-1} resulting from the -CH_2 stretching of the octadecyl chain.

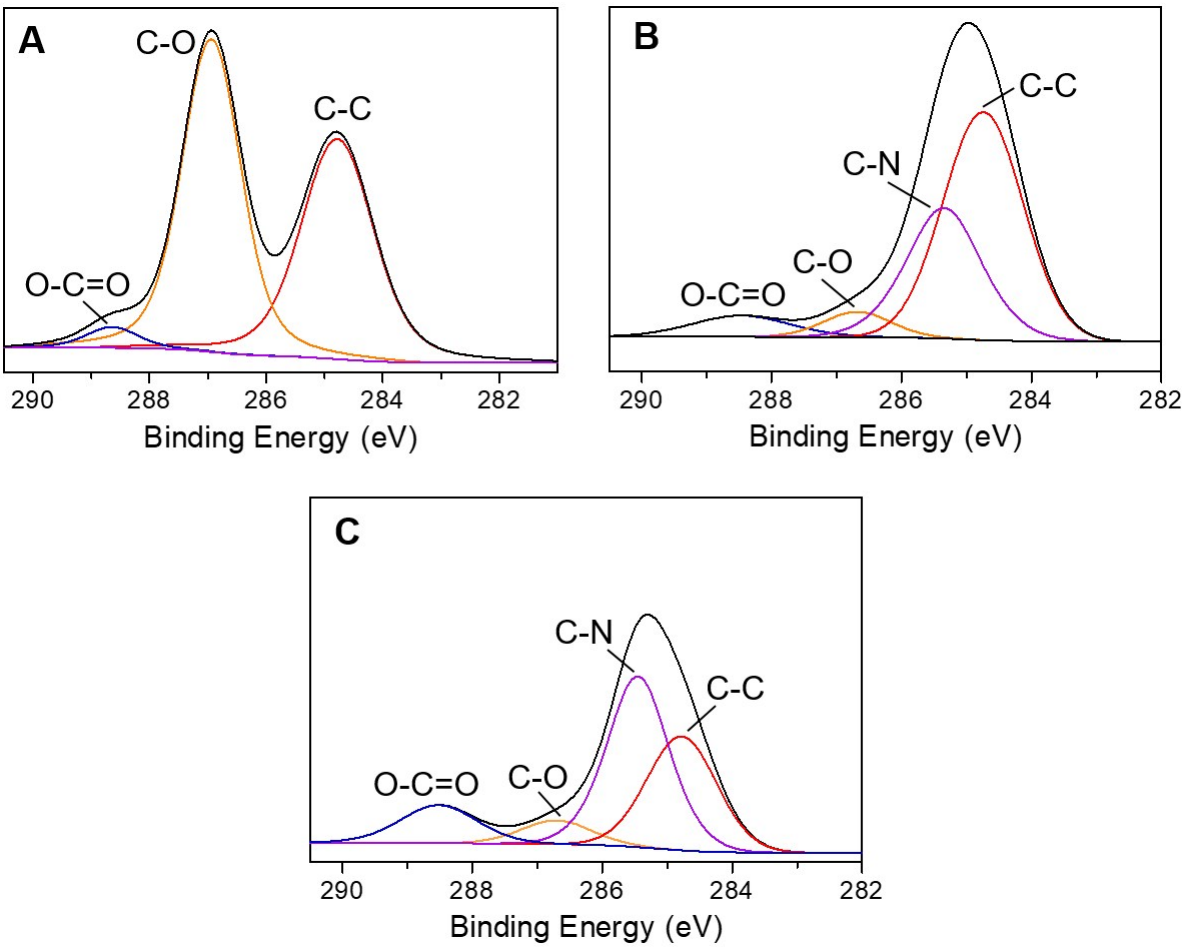

Fig. S6. C1s XPS spectra of GO (**A**), C_{18}-GO-C_{18} (**B**) and JG (**C**). From (**A**), GO shows dominant C-C, C-O, and O-C=O peaks at 284.8, 286.8, and 288.8 eV, respectively. From (**B**), peak fitting of the C1s bands of C_{18}-GO-C_{18} yields four main components at 284.8, 285.6, 286.8, and 288.8 eV, assigning to C-C, C-N, C-O, and O-C=O bonds, respectively. Comparing with GO, the C-O signal decreases and the C-N signal increases due to the reaction between carboxylic or epoxy groups and amine. From (**C**), JG shows C-C, C-N, C-O, and O-C=O peaks at 284.8, 285.6, 286.8 and 288.8 eV, respectively. Comparing with C_{18}-GO-C_{18}, the ratio between C-N and C-C (O-C=O and C-O) is higher due to the introduction of EDTA-silane. Furthermore, we can also obtain the atomic percentages from the XPS measurements, which enables a rough estimate of the ratio of ODA to EDTA in the JG (the results are given in Table S1).

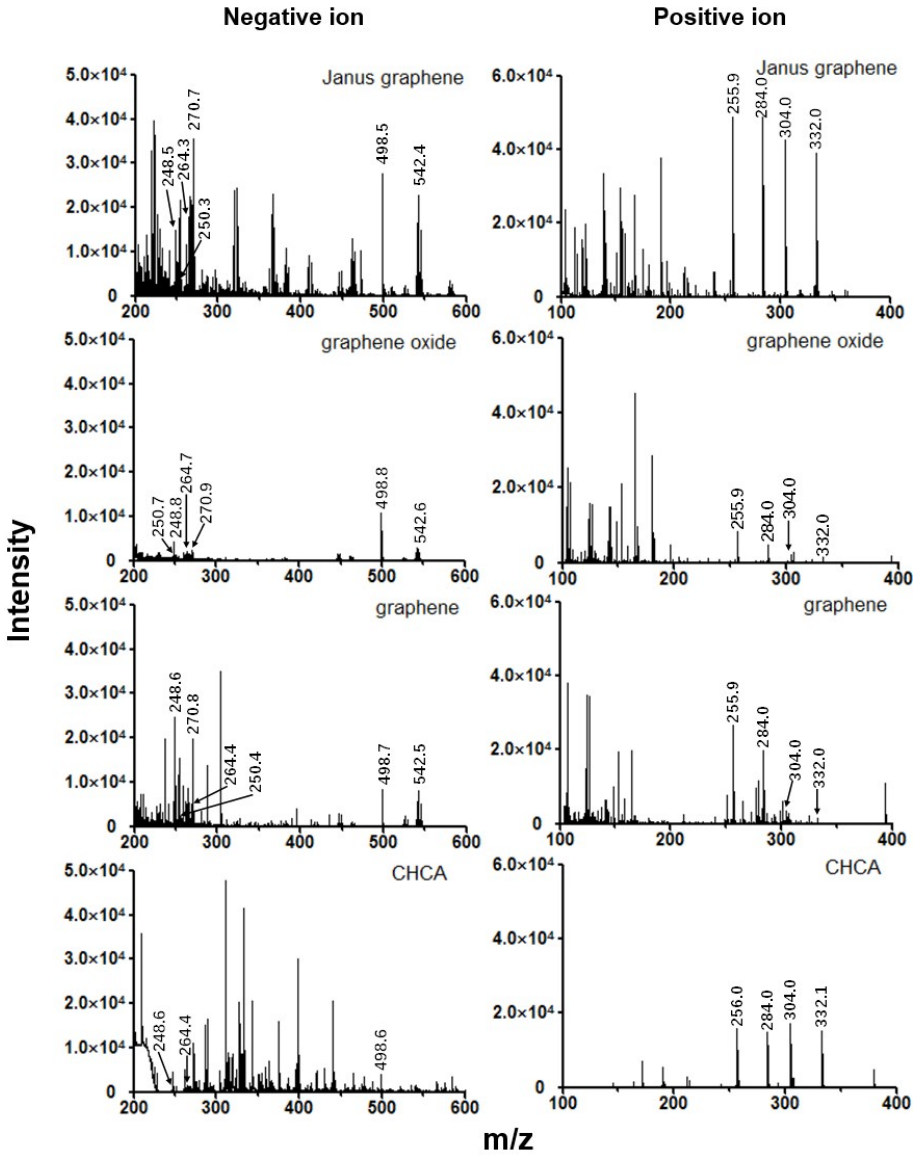

Fig. S7. Comparison of different materials as matrices in MALDI-TOF MS detection of typical toxic organic compounds (BPS, BDE-47, PCP, E2, PFOS, TBBPA, TDBAC, DDBAC, CTAB and TTAB). The left and right column denote the mass spectra obtained in negative and positive ion mode, respectively. The samples were incubated with the matrix for 3 h before the analysis. Analyte concentration: BPS, 10 μg/mL; BDE-47, 50 μg/mL; PCP, 10 μg/mL; E2, 50 μg/mL; PFOS, 1 μg/mL; TBBPA, 50 μg/mL; TTAB, 5 μg/mL; CTAB, 5 μg/mL; DDBAC, 10 μg/mL; and TDBAC, 10 μg/mL.

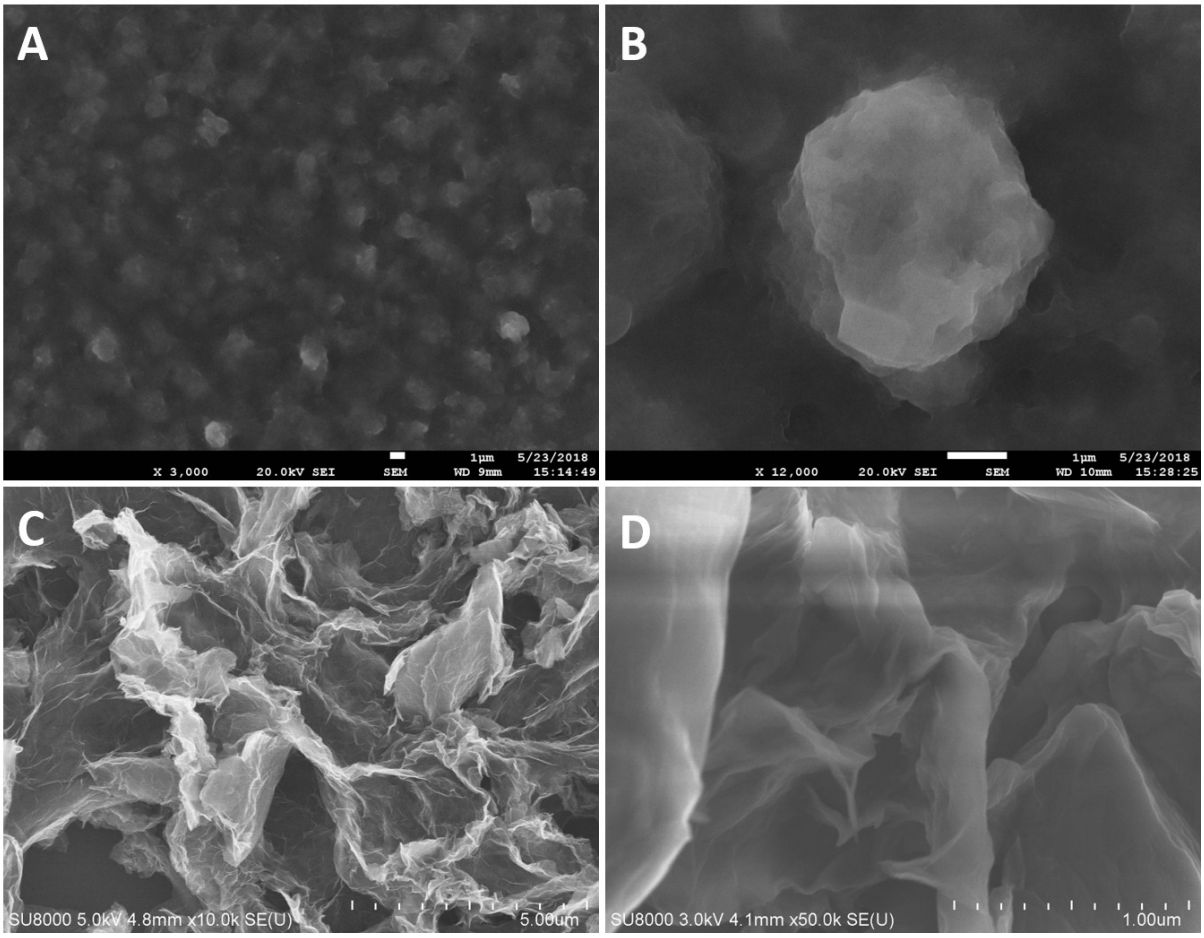

Fig. S8. FE-SEM images of Janus graphene matrix at low- (**A**) and high-amplification (**B**), unmodified graphene matrix (**C**), and GO matrix (**D**) on the MALDI target. From (**A**), interestingly, we find that the JG can form well distributed and ordered self-assembles on the MALDI target. We ascribe this phenomenon to the amphiphilic nature of JG, that is, the EDTA side is polar and the C_{18} side is non-polar. Therefore, it should behave like surfactants that can form micelles or vesicles in the aqueous solution. The JG self-assembles, with a size of about 5 μm, show a good monodispersity with no overlapping or crosslinking. The underlying mechanism needs further investigations in future studies. Furthermore, it should be noted that such a structure can improve the homogeneity of the JG film on the MALDI target and prevent it from irreversible aggregates, which thus may be favorable for the MALDI-TOF MS detection. By contrast, as shown in (**C**), graphene is found to easily form multilayered aggregates on the MALDI target to leave a part of the MALDI target surface uncovered by the matrix, which may seriously impair the reproducibility of the MALDI-TOF MS detection. For GO matrix (**D**), the homogeneity of the film, although with some wrinkles, is much better than the G matrix. Unlike JG, no self-assembles are observed with the GO matrix.

References for SI

1. Q. Liu, J. Shi, M. Cheng, G. Li, D. Cao and G. Jiang, *Chem. Commun.*, 2012, **48**, 1874-1876.
2. J. Hong, C. Liu, X. Deng, T. Jiang, L. Gan and J. Huang, *RSC Adv.*, 2016, **6**, 89221-89230.
3. S. Hou, S. Su, M. L. Kasner, P. Shah, K. Patel and C. J. Madarang, *Chem. Phys. Lett.*, 2010, **501**, 68-74.
4. J. Zhang, Z. Zhu, Y. Tang and X. Feng, *J. Mater. Chem. A*, 2013, **1**, 3752-3756.
5. C. J. Madadrang, H. Y. Kim, G. Gao, N. Wang, J. Zhu, H. Feng, M. Gorring, M. L. Kasner and S. Hou, *ACS Appl. Mater. Interf.*, 2012, **4**, 1186-1193.